

Statistical study of defects caused by primary knock-on atoms in fcc Cu and bcc W using molecular dynamics

M. Warriar^a, U. Bhardwaj^a, H. Hemani^a, R. Schneider^c, A. Mutzke^c, M. C. Valsakumar^d

^a*Computational Analysis Division, BARC, Visakhapatnam, Andhra Pradesh, India - 530012*

^b*Computational Science, Ernst-Moritz-Arndt University, D-17489 Greifswald, Germany*

^c*Max-Planck-Institut für Plasmaphysik, D-17491 Greifswald, Germany*

^d*School for Engineering Science and Technology, University of Hyderabad, Gacchibowli,
Hyderabad, Telangana State - 500046*

Abstract: We report on molecular Dynamics (MD) simulations carried out in fcc (Cu) and bcc metals (W) using the Large-scale Atomic/Molecular Massively Parallel Simulator (LAMMPS) code to study (i) the statistical variations in the number of Frenkel Pairs produced by energetic primary knock-on atoms (PKA) (0.1-5 keV) directed in random directions and (ii) the in-cascade cluster size distributions. It is seen that more than 100 random directions have to be explored for the variance in the number of Frenkel pairs produced to become steady in the case of fcc Cu, whereas for bcc W at least 60 random directions need to be explored. It is also seen that most of the interstitials are single in all cases. The number of Frenkel pairs produced in the MD simulations are compared with that from the Binary Collision Approximation Monte Carlo (BCA-MC) code SDTRIM-SP and the results from the NRT model. It is seen that a proper choice of the damage energy, i.e. the energy required to create a stable interstitial is essential for the BCA-MC results to match the MD results. On the computational front it is seen that in-situ processing saves the need to input / output (I/O) atomic position data of several tera-bytes when exploring 1000 random directions and there is no difference in run-time because the extra

run-time in processing data is offset by the time saved in I/O.

JNM keywords:

PACS codes:

* *Corresponding author e-mail:* Manoj.Warrier@gmail.com

* *Corresponding author address:* Computational Analysis Division, BARC, Visakhapatnam, Andhra Pradesh, India - 530012

1 Introduction

Primary damage of materials due to neutron irradiation occurs via energetic cascades caused by energetic primary knock-on atoms (PKA) created by the energetic neutron as it passes through the material. These cascades result in creation of Frenkel Pairs (interstitials and vacancies). The interstitials and vacancies diffuse and recombine to (I) nullify the damage when an interstitial recombines with a vacancy, (II) form interstitial clusters when two or more interstitials recombine, and (III) form vacancy clusters when several vacancies come together. The long term changes in micro-structure and composition of the irradiated material is a multi-scale problem [1–5].

The primary cascades are modeled either by Molecular Dynamics ([1] and references therein) or by binary collision approximation (BCA) Monte Carlo Simulations [7–10]. BCA neglects many body effects, and is valid only at energies > 100 eV. Moreover, in BCA there is ambiguity in identifying a displaced atom. An atom is considered to be

displaced in either of two ways: (1) if it has an energy greater than a specified displacement energy E_d , i.e., the threshold energy that an atom needs to be a stable interstitial [7,10], or (2) if it is at a distance greater than a specified distance from a vacancy, called the vacancy recapture radius. This vacancy recapture radius is obtained from considerations of crystal mechanical stability [11] and varying criteria are used ($1.53a$ in, [8] and $2.5a$ in, [9] for Fe, where a is the lattice parameter of the target material). There is also ambiguity in the value of the displacement energy E_d , [7,12–14].

MD simulations of collisional cascades takes into consideration many body effects and therefore is more accurate than BCA Monte Carlo codes [15]. MD also provides insight into the atomistic details like in-cascade clustering of interstitials, their configuration and also their dynamic evolution up-to several nanoseconds. However, MD has inherent limitations in the number of atoms it can simulate (at most a fraction of a micron on advanced supercomputers), the time it can span (around 10 nanoseconds) and the huge computational costs involved. MD also does not account for electronic stopping losses [16]. Special procedures have to be introduced in MD codes to take this into account [17].

Stoller et al., have carried out several hundred MD simulations along the $\langle 100 \rangle$, $\langle 110 \rangle$, $\langle 111 \rangle$ and $\langle 135 \rangle$ directions of Fe in the energy range from 0.1 to 50 keV, to statistically analyze MD cascades in bcc iron at 100 K, [15]. Randomness was introduced in their simulations by carrying out NPT simulations to equilibrate the target to different times, choosing a different PKA location, or a combination of both. More recently Warriar et al., carried out MD simulations of PKAs directed along 1000 random directions in Fe(90%)-Cr(10%) alloy in the energy range of 0.1 to 5 keV [18]. They showed that at least a hundred random

directions have to be explored for the standard deviation in the number of displaced atoms to stabilize. In this work we direct the PKA in 200 random directions for bcc W and fcc Cu in the energy range of 0.1-5 keV in order to (a) obtain the number of Frenkel pairs produced, (b) obtain the fraction of in-cascade clustering that occurs and the cluster size distributions and (c) compare the results from MD simulations with BCA-MC code SDTRIM-SP and with the NRT model.

In the next section we describe the simulations and methods used. Then results from the MD simulations on number of Frenkel pairs and clustering are presented in Section.3. In Section.4 the results from the BCA-MC code are compared with the MD results. Finally we present the conclusions from the study.

2 Description of the Simulations and Methods

Cascade simulations were carried out with both MD and BCA-MC codes. The Large-scale Atomic / Molecular Massively Parallel Simulator (LAMMPS) code, [19] was used to carry out the MD simulations. Table.1 and Table.2 show the size of the cubic simulation box used for the Cu and W simulations in the second column along with other direction averaged results in the results section. The PKA is a lattice atom lying at the center of the cubic box. For Cu and W, 200 MD simulations of the PKA in random directions at energies of 1, 2, 3, 4, and 5 keV respectively were carried out. At each energy, a new seed for the random number generator is used to obtain the 200 random directions thereby making the sequence of directions explored unique.

The embedded atom potential (EAM) developed by Foiles, et al [21] was used for the Cu simulations. For W, the EAM/alloy potential implemented by G. Ziegenhain based on the method by Zhou et al. [22] was used. Note that these potentials have not been stiffened to properly account for short range interactions. Periodic boundary conditions are specified in all three directions and the atoms in the outermost unit cells on all faces of the cube are kept fixed. Scoping runs using a Nosé-Hoover NPT ensemble at 300 K established that equilibrium was reached in the various systems in 8-10 ps and the cascade dynamics in the energy range explored saturates within 5 ps [18]. Adaptive time stepping was used with the criterion for the time step being decided by either a minimum time step of 0.01 fs or the time required by the fastest atom to move being 0.1 \AA , whichever is smaller. The cascade simulations were then run for 6 ps using a micro-canonical ensemble.

For the BCA-MC simulations, the SDTRIM-SP code [10] was used to simulate the PKA cascades in the same energy range as that of the MD simulations. For comparison with MD results and with the NRT model, the following cases were explored in each series of the BCA-MC simulations:

- (1) Electronic stopping was switched off since the MD simulations do not take this into consideration.
- (2) The displacement energy E_d was fixed at 40 eV, since this is the standard recommended in the NRT model [11] with electronic stopping on. The default value of E_d in SDTRIM-SP for W is 38 eV, and this was used.
- (3) E_d as recommended in [7] for Cu (19 eV) and a value for E_d for W from MD calculations [14], 98 eV, was used with electronic stopping on.

The procedure for finding the surviving number of Frenkel Pairs has been described in [18]. Essentially, the distance between the initial position (perfect lattice site) and the current positions of each atom is monitored and if it is greater than a specified value (r_{disp}), it is considered to be displaced. The distance between each of the displaced atoms and vacancy sites (initial positions of the displaced atoms) are then calculated. If this distance is less than a specified value (r_{rec}) for a displaced atom - vacancy pair, the displaced atom is considered to have occupied the vacant lattice site. The surviving displaced atoms that do not recombine with a vacancy are then analyzed to see if they are dumbbells or crowdions and the correct number of displaced atoms is calculated [1]. The range of the PKA and the maximum displacement of the recoils (displaced atoms) are also monitored.

The final steady defects may form clusters of different sizes. The distance between the defects is used as a measure to group them into clusters. Initially, every defect is considered to be as a cluster of size one. The union of two clusters having same kind of defects (interstitial/vacancy) is carried out if the distance between any of the defects in the two is less than a certain value. This distance is approximated by finding out the preferred distance between the nearest defect of a kind from the MD simulations of cascades. This distance can be seen as the distance at which the energy of the bound system (defects) is minimum, hence the defects tend to cluster at this distance [1]. The above clustering method is used to verify clustering at 1 to 5 NN (nearest neighbor) distances and a suitable distance, hitherto referred to as the clustering distance, is chosen for vacancy and interstitial cluster distributions.

3 Results From the MD Simulations

The evolution of the number of Frenkel pairs as a function of time for Cu and W are shown for a random PKA at each of the energy ranges explored in Fig.1 and Fig.2 respectively. It is seen that the time scales for the collision cascade dynamics is a few ps and the number of Frenkel pairs saturate by 5 ps. At lower PKA energy, the saturation occurs faster. After saturation, the number of Frenkel pairs are corrected for over-counting due to dumbbell and crowdion configurations and these values are output in Table.1 and Table.2 for Cu and W respectively. Table.1 and Table.2 shows the average number of Frenkel pairs, the average range of the PKA, the average range of the maximum displacement and the variance of these parameters over the 200 random directions explored.

The standard deviation in the number of Frenkel Pairs as a function of the number of PKA launched in random directions in the energy range 1-5 keV is shown in Fig.3 and Fig.4 respectively. For the N^{th} PKA, the first N data points are used to find the standard deviation. It is seen that around 100-200 random directions have to be sampled for the standard deviation in Cu to saturate and around 60-100 random directions have to be explored for the standard deviation in W to saturate.

The normalized number of clusters of interstitials and vacancies at different nearest neighbor (NN) distances for the 200 random directions have been explored. Their values for Cu and W at each of the energy range explored are shown in Fig.5, Fig.6, Fig.7 and Fig.8 respectively. From this it is clear that most of the interstitials and vacancies are single ($> 6NN$). Note that most of the interstitials lie within 1NN distance in both Cu and in W

and most of the vacancies are between 1NN-2NN.

Dumbbells and crowdions are observed for both, Cu and W, as shown in Fig.9 and Fig.10 respectively. Fig.9 is for a 2 keV PKA in Cu and Fig.10 is for a 5 keV PKA in W. Bigger clusters are seen in W and many of these are ring shaped, whereas this is not the case in Cu (even at 5 keV). Sub-cascades are found in Cu even at these low energies of PKA, unlike in W where sub-cascades are not seen even at 5 keV.

The direction averaged distribution of interstitials and vacancies around a PKA location for Cu and W are shown in Fig.11, Fig.12, Fig.13 and Fig.14 respectively. These can be useful inputs for simulations at the higher scales. !! Describe trends, and explain spike in vacancy spot!!

4 Comparison of MD results with BCA-MC

Fig.15 and Fig.16 compares the surviving number of defects from our MD simulations for Cu and W respectively with the three cases for which the BCA-MC simulations were carried out and with the prediction from the NRT formula [11] (which uses $E_d = 40$ eV). For W, the value of E_d in SDTRIM-SP is 38 eV, which is close to the NRT value. Despite this, the results for the number of displaced atoms predicted by SDTRIM-SP is much higher than that from the MD simulations and the predictions of the NRT model. Therefore for W we use a value of E_d obtained from the MD studies of Setyawan et al. [14] and get a much closer match between the BCA-MC and MD simulations. For Cu, we get a good match between SDTRIM-SP results with a value of $E_d = 40$ eV. Note that the PKA

energies for the MD simulation results are the corrected values which take into account losses due to electronic stopping as recommended in [1]. It is seen that our results for Cu and W follow an empirical power law proposed by Bacon et al. [23], $N_{disp} = A E_{MD}^m$, with $A = 8.0$ and $m = 1.05$ for Cu and $A = 3.8$ and $m = 0.75$ for W.

The BCA-MC results show a much higher number of displaced atoms than that predicted by MD and do not match the MD results unless a higher value of E_d is chosen. E_d as per definition is *the energy required to create a stable interstitial*. This however does not take into consideration that the stable interstitial created is with respect to the vacancy formed at its initial position (we call this its original vacancy). It may however be within the vacancy recapture radius of another vacancy which was created as part of the cascade and may recombine with it. This is not taken into consideration in the SDTRIM-SP simulations. This brings into focus the second method of identifying a stable displaced atom as mentioned in the introduction, viz, have a vacancy recapture radius and if the interstitial is within this radius of any vacancy created by the cascade, it and the vacancy annihilate each other. Therefore, it is recommended that in BCA-MC simulations, a E_d obtained from MD be used and the final recoil positions be tested for stability by specifying a vacancy recapture radius. The latter recommendation has not been proved in this paper, but it seems desirable to account for the recombination of interstitials with vacancies other than its original vacancy.

5 Conclusions

Using molecular dynamics simulations, we show that collision cascades of at least around 100-200 random directions of PKA in a crystal have to be sampled for the standard deviation in the number of Frenkel pairs produced to saturate in fcc Cu and around 60-100 random directions have to be explored for bcc W for PKA energy range 1-5 keV. It is seen that most of the interstitials and vacancies created are single for both Cu and W. The fraction of in-cascade clusters of interstitials and vacancies are presented. The direction averaged distribution of vacancies and interstitials around the starting point of a PKA is also shown for both, Cu and W in the PKA energy range 1-5 keV. All these data are useful inputs to higher scale simulations of radiation damage.

Similar collision cascade simulations were also carried out using the BCA-MC code SDTRIM-SP and the results were compared with MD simulations. It is seen that the BCA-MC results have a better match with the MD results when a value of the displacement energy, E_d , obtained from MD simulations is used in the BCA-MC simulations. Moreover it is desirable to test the final recoil positions for stability against other vacancy sites by specifying a vacancy recapture radius.

Acknowledgments

We would like to thank N. Sakthivel and his team from the supercomputing centre and A. Majalee, all from C.A.D, BARC-Visakhapatnam for the supercomputing cluster support.

References

- [1] R.E. Stoller, "Primary radiation damage formation", *Comprehensive Nuclear Materials*, **1** (2012) 293-332.
- [2] R.E. Stoller and L.K. Mansur, "An assessment of radiation damage models and methods", *ORNL Report ORNL/TM-2005/506* **2005**.
- [3] P.R. Monasterio, B.D. Wirth and G.R. Odette, "Kinetic Monte Carlo modeling of cascade aging and damage accumulation in Fe-Cu alloys", *J. Nucl. Mater.* **361** 127–140 (2007).
- [4] C. Björkas, K. Nordlund and M.J. Caturla, "Influence of the picosecond defect distribution on damage accumulation in irradiated α -Fe", *Phys. Rev. B* **85**, 024105 (2012).
- [5] C.S. Becquart, C. Domain, LO. Malerba, M. Hou, "The influence of the internal displacement cascades structure on the growth of point defect clusters in radiation environment", *Nucl. Instrum. and Meth. B* **228** (2005) 181-186.
- [6] C. Domain, C. S. Becquart and L. Malerba, "Simulation of radiation damage in Fe alloys: an object kinetic Monte Carlo approach", *J. Nucl. Mater.* **335** (2004) 121-145.
- [7] W. Eckstein, Computer Simulations of Ion-Solid Interactions em Springer series in Material Science 10 *Springer Verlag* (1991).
- [8] M.T. Robinson and I.M. Torrens, "Computer simulation of atomic-displacement cascades in solids in the binary-collision approximation", *Phys. Rev. B* **9** 5008–5024 (1974).
- [9] M.T. Robinson, "Slowing down time of energetic atoms in solids", *Phys. Rev. B.* **40** (16) 10717–10726 (1989).

- [10] A. Mutzke, R. Schneider, W. Eckstein and R. Dohmen, "SDTrimSP Version 5.00", *Max-Planck Institute for Plasmaphysics Report IPP 12/8* (2011).
- [11] M.J. Norgett, M.T. Robinson and I.M. Torrens, "A proposed method of calculating displacement dose rates", *Nucl. Eng. and Design* **33** 50–54 (1975).
- [12] K. Nordlund, J. Wallenius and L. Malerba, "Molecular dynamics simulations of threshold displacement energies in Fe", *Nucl. Instrum. and Meth. B* **246** (2006) 322332.
- [13] N. Juslin, K. Nordlund, J. Wallenius and L. Malerba, "Simulation of threshold displacement energies in FeCr", *Nucl. Instrum. and Meth. B*, **255** (2007) 75-77.
- [14] W. Setyawan, Aaron P. Selby, N. Juslin, Roger E. Stoller, Brian D. Wirth, and Richard J. Kurtz, "Cascade morphology transition in bcc metals", *arxiv preprint, cond-mat.mtrl-sci, 1412.7452v1* (2014).
- [15] R.E. Stoller and A.F. Calder, "Statistical analysis of a library of molecular dynamics cascade simulations in iron at 100 K", *J. Nucl. Mater.* **283-287** (5), 746–752 (2000).
- [16] A.M. Rutherford and D.M. Duffy, "The effect of electronion interactions on radiation damage simulations", *J. Phys. Condens. Matter*, **19** (2007) 496201.
- [17] D.M. Duffy and A.M. Rutherford, "Including the effects of electronic stopping and electronion interactions in radiation damage simulations", *J. Phys. Condens. Matter*, **19** (2007) 016207.
- [18] M. Warriar and M.C. Valsakumar, "Study of molecular dynamics collision cascades in 1000 random directions in crystal Fe(90%)Cr(10%) in the energy range 0.1 to 5 KeV", *Fusion Sci. Tech.* **65** #2 (2014) 222-228.

- [19] S.J. Plimpton, "Fast Parallel Algorithms for Short-Range Molecular Dynamics", *J. Comp. Phys.* **117** 1–19 (1995).
- [20] A. Stukowski, B. Sadigh, P. Erhart and A. Caro, "Composition-dependent interatomic potentials: A systematic approach to modelling multicomponent alloys", *Modeling Simul. Mater. Sci. Eng.* **17**, 075005 (2009).
- [21] S. M. Foiles, M. I. Baskes, and M. S. Daw, "Embedded-atom-method functions for the fcc metals Cu, Ag, Au, Ni, Pd, Pt, and their alloys", *Phys. Rev. B* **33** (2007) 7983.
- [22] X.W. Zhou, H.N.G. Wadley, R.A. Johnson, D.J. Larson, et al., "Atomic scale structure of sputtered metal multilayers", *Acta Mater.* **49**, #19, (2001) 4005.
- [23] D.J. Bacon, A.F. Calder, F. Gao, V.G. Kapinos and S.J. Wooding, "Computer simulation of defect production by displacement cascades in metals", *Nucl. Instrum. and Meth. B*, **102** 37 (1995).

List of Figures

- 1 Total number of Frenkel Pairs as a function of time for Cu PKA at energy 1,2,3,4 and 5 keV. This plot does not account for double counting due to "dumbbells" and "crowdions". The values in Table.1 accounts for these. 17
- 2 Total number of Frenkel Pairs as a function of time for W PKA at energy 1,2,3,4 and 5 keV. This plot does not account for double counting due to "dumbbells" and "crowdions". The values in Table.2 accounts for these. 18
- 3 Variation of standard deviation in the number of Frenkel pairs in Cu as a function of the number of the PKA launched in random directions at energies 1-5 keV 19
- 4 Variation of standard deviation in the number of Frenkel pairs in W as a function of the number of the PKA launched in random directions at energies 1-5 keV 20
- 5 Histogram of the normalized interstitials clustering at different values of nearest neighbor (NN) in Cu for PKA energies of 1-5 keV 21
- 6 Histogram of the normalized vacancy clustering at different values of nearest neighbor (NN) in Cu for PKA energies of 1-5 keV 22
- 7 Histogram of the normalized interstitials clustering at different values of nearest neighbor (NN) in W for PKA energies of 1-5 keV 23

8	Histogram of the normalized vacancy clustering at different values of nearest neighbor (NN) in W for PKA energies of 1-5 keV	24
9	A picture of the Frenkel pairs in Cu at PKA energy of 2 keV. Vacancies are in red and the interstitials are in green color. Note that dumbbells and complex vacancy clusters are common in Cu, even at low energies of PKA.	25
10	A picture of the Frenkel pairs in W at PKA energy of 5 keV. Vacancies are in red and the interstitials are in green color. It shows dumbbells, crowdions and ring like arrangement of interstitial clusters.	26
11	Distribution of the interstitials as a function of distance from the origin of the PKA for energies 1-5 keV in Cu	27
12	Distribution of the Vacancies as a function of distance from the origin of the PKA for energies 1-5 keV in Cu	28
13	Distribution of the interstitials as a function of distance from the origin of the PKA for energies 1-5 keV in W	29
14	Distribution of the Vacancies as a function of distance from the origin of the PKA for energies 1-5 keV in W	30
15	Variation of the number of Frenkel Pairs as a function of the energy of PKA from MD simulations, NRT Model and SDTRIM-SP simulations for the three cases, viz. without electronic stopping, with electronic stopping, with $E_d = 40$ eV for Cu	31

16	Variation of the number of Frenkel Pairs as a function of the energy of PKA from MD simulations, NRT Model and SDTRIM-SP simulations for the three cases, viz. without electronic stopping, with electronic stopping, with $E_d = 98$ eV for W	32
----	--	----

List of Tables

1	Direction averaged values of N_{disp} , Sample size in terms of number of unit cells of size 3.615 Å, the number of Frenkel Pairs, $PKAD$, the range of the PKA and $MaxD$, the maximum displacement for Cu. The value after the \pm sign is the standard deviation of these quantities.	18
2	Direction averaged values of N_{disp} , Sample size in terms of number of unit cells of size 3.615 Å, the number of Frenkel Pairs, $PKAD$, the range of the PKA and $MaxD$, the maximum displacement for W. The value after the \pm sign is the standard deviation of these quantities.	19

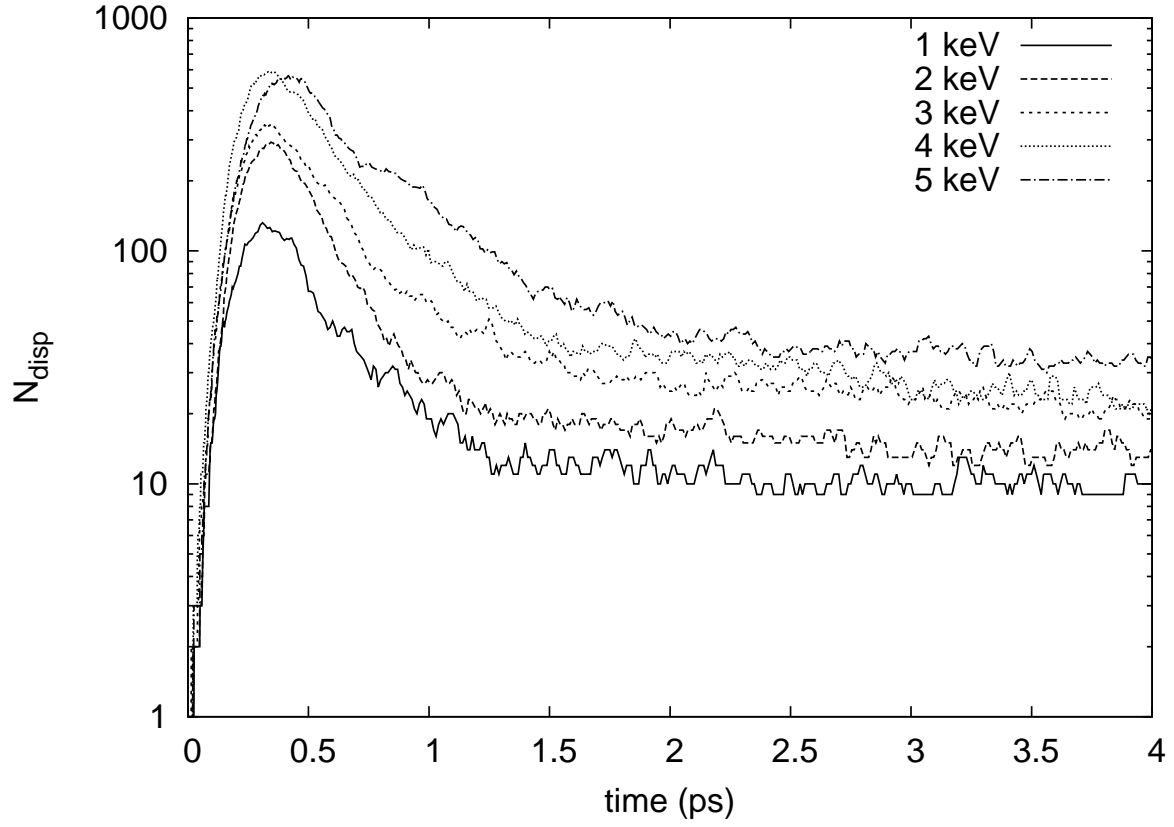


Fig. 1. Total number of Frenkel Pairs as a function of time for Cu PKA at energy 1,2,3,4 and 5 keV. This plot does not account for double counting due to "dumbbells" and "crowdions". The values in Table.1 accounts for these.

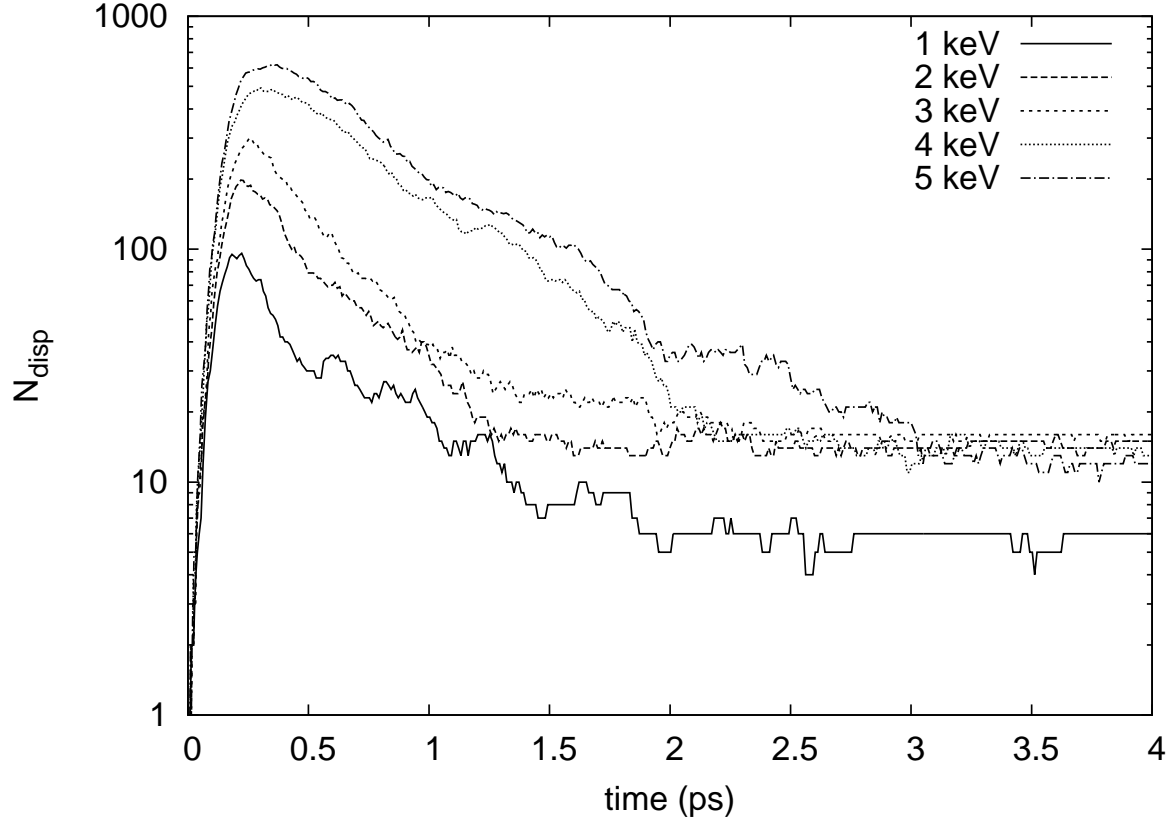


Fig. 2. Total number of Frenkel Pairs as a function of time for W PKA at energy 1,2,3,4 and 5 keV. This plot does not account for double counting due to "dumbbells" and "crowdions". The values in Table.2 accounts for these.

Table 1

Direction averaged values of N_{disp} , Sample size in terms of number of unit cells of size 3.615 Å, the number of Frenkel Pairs, $PKAD$, the range of the PKA and $MaxD$, the maximum displacement for Cu. The value after the \pm sign is the standard deviation of these quantities.

E_{PKA} (keV)	$n_x=n_y=n_z$	Sample Size	N_{disp}	$PKAD$ (Å)	$MaxD$ (Å)
1	60	1000	7 ± 2	42.84 ± 25.32	51.6 ± 22.1
2	80	500	14 ± 3	62.67 ± 35.29	75.86 ± 29.4
3	100	500	20 ± 3	80.62 ± 45.71	97.03 ± 39.74
4	110	200	27 ± 4	88.08 ± 48.65	107.69 ± 40.84
5	110	200	34 ± 4	102.99 ± 59.12	122.01 ± 52.38

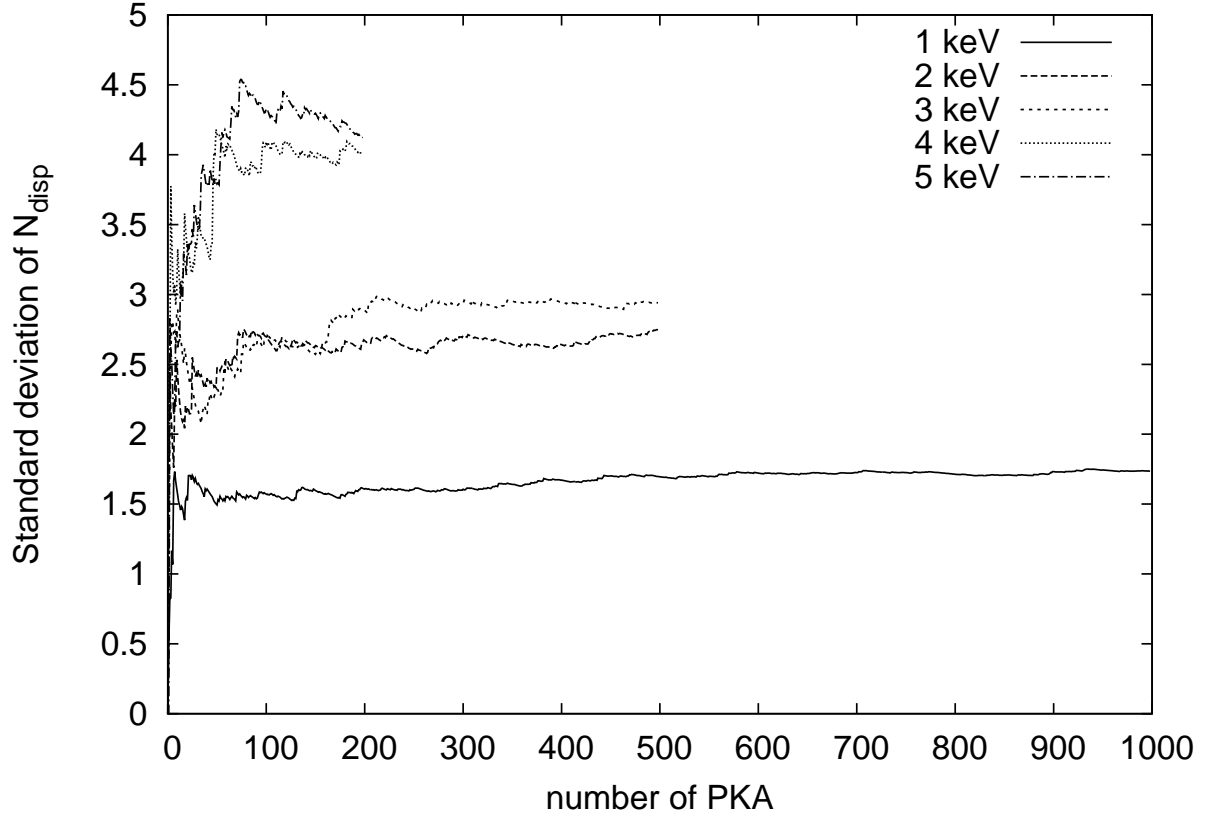


Fig. 3. Variation of standard deviation in the number of Frenkel pairs in Cu as a function of the number of the PKA launched in random directions at energies 1-5 keV

Table 2

Direction averaged values of N_{disp} , Sample size in terms of number of unit cells of size 3.615 Å, the number of Frenkel Pairs, $PKAD$, the range of the PKA and $MaxD$, the maximum displacement for W. The value after the \pm sign is the standard deviation of these quantities.

E_{PKA} (keV)	$n_x=n_y=n_z$	Sample Size	N_{disp}	$PKAD$ (Å)	$MaxD$ (Å)
1	50	200	3 ± 1	9.41 ± 2.68	10.17 ± 2.15
2	50	200	5 ± 2	15.54 ± 5.84	16.71 ± 5.02
3	50	190	6 ± 2	17.53 ± 9.43	18.91 ± 9.21
4	50	200	9 ± 2	29.32 ± 14.69	31.00 ± 13.55
5	50	200	11 ± 3	34.66 ± 15.94	36.52 ± 14.87

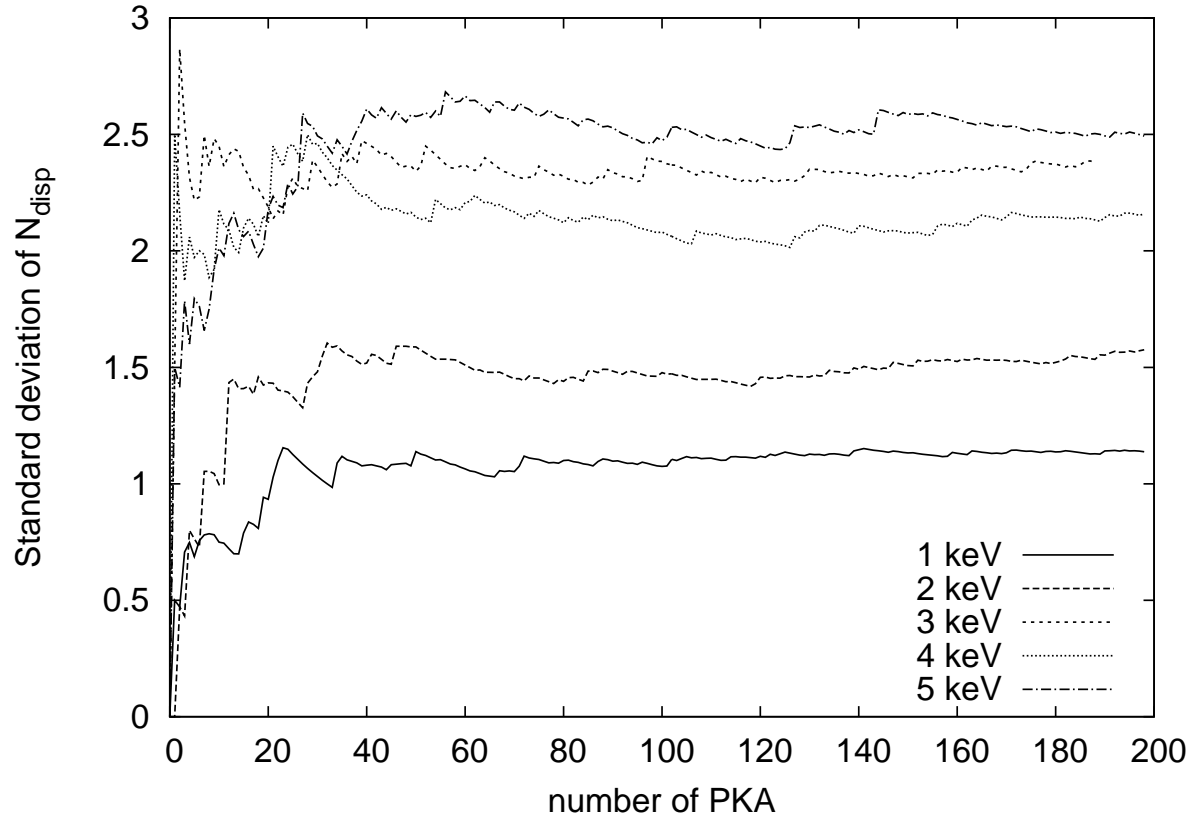


Fig. 4. Variation of standard deviation in the number of Frenkel pairs in W as a function of the number of the PKA launched in random directions at energies 1-5 keV

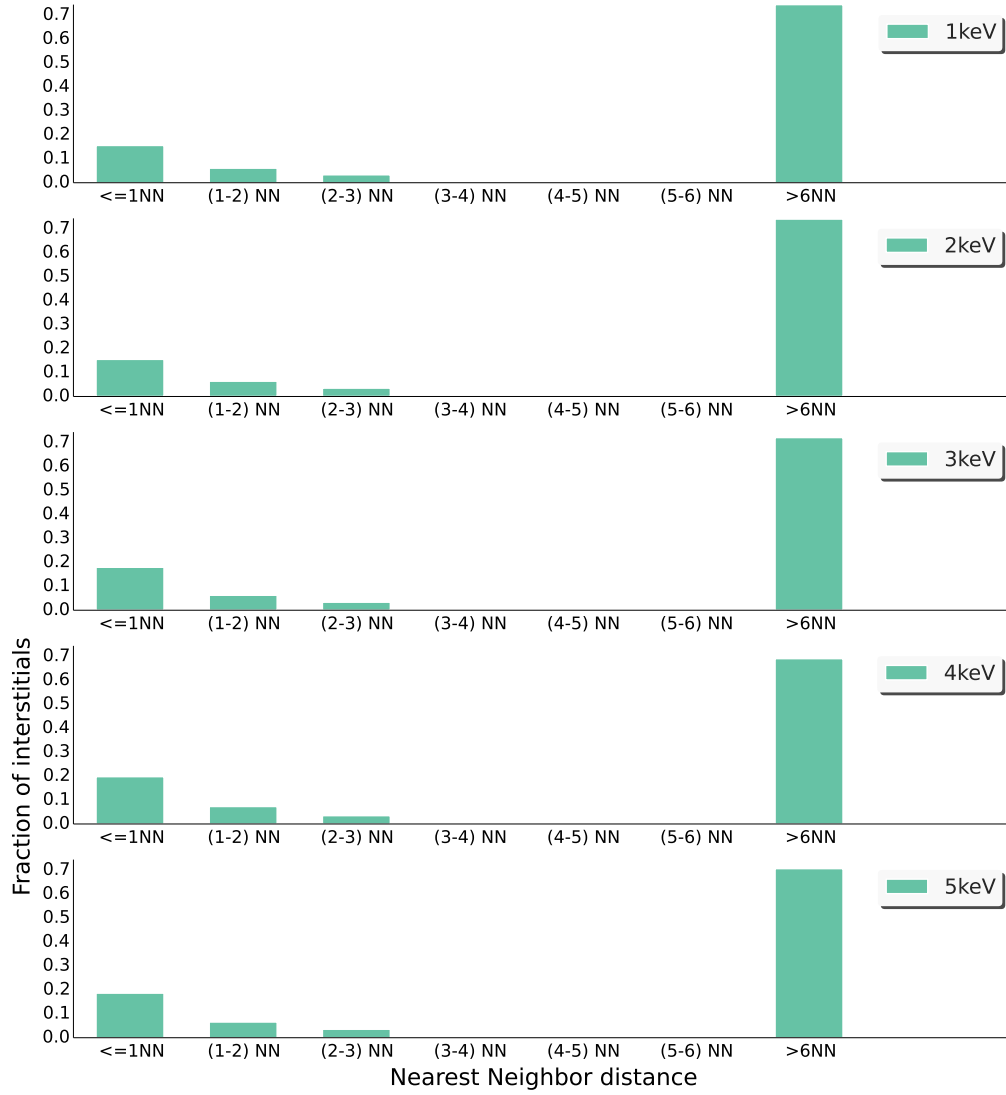


Fig. 5. Histogram of the normalized interstitials clustering at different values of nearest neighbor (NN) in Cu for PKA energies of 1-5 keV

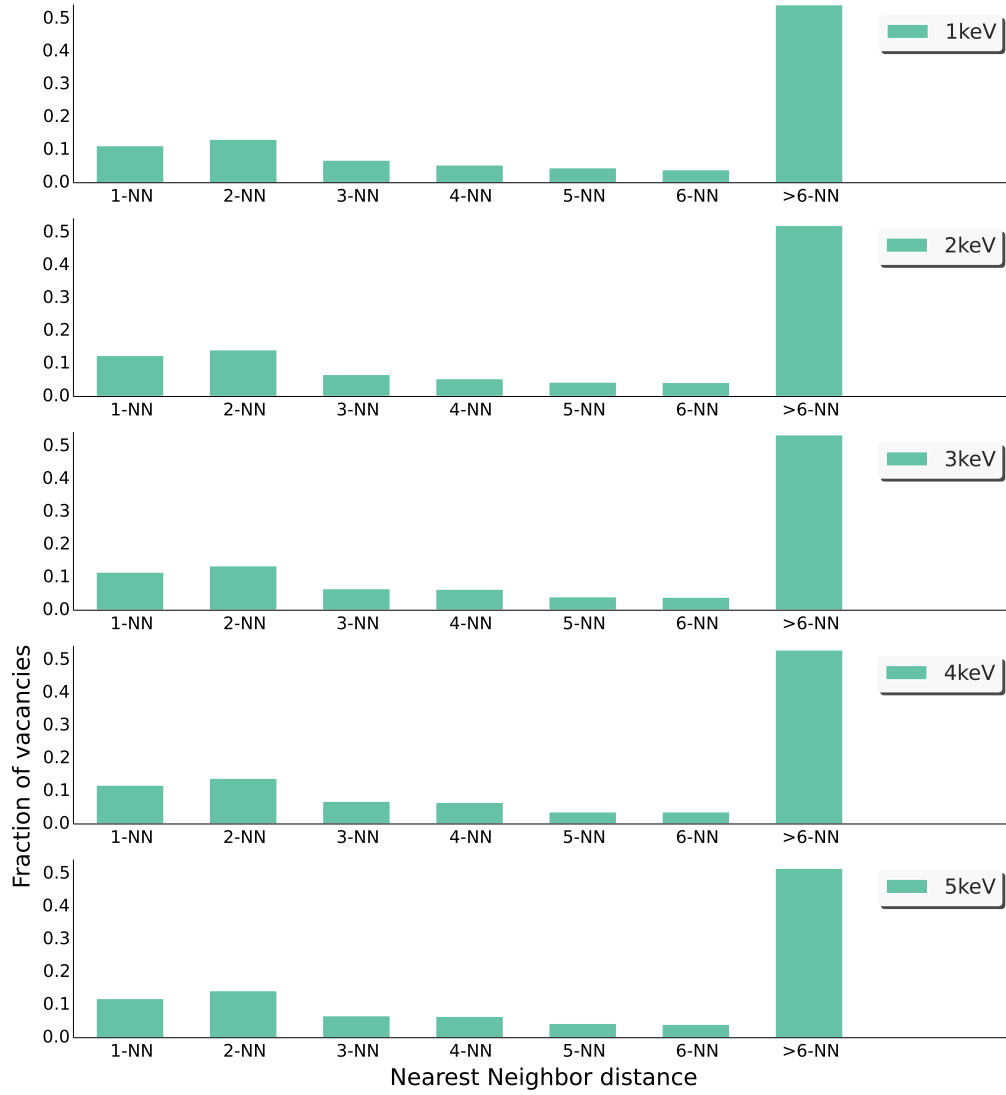


Fig. 6. Histogram of the normalized vacancy clustering at different values of nearest neighbor (NN) in Cu for PKA energies of 1-5 keV



Fig. 7. Histogram of the normalized interstitials clustering at different values of nearest neighbor (NN) in W for PKA energies of 1-5 keV



Fig. 8. Histogram of the normalized vacancy clustering at different values of nearest neighbor (NN) in W for PKA energies of 1-5 keV

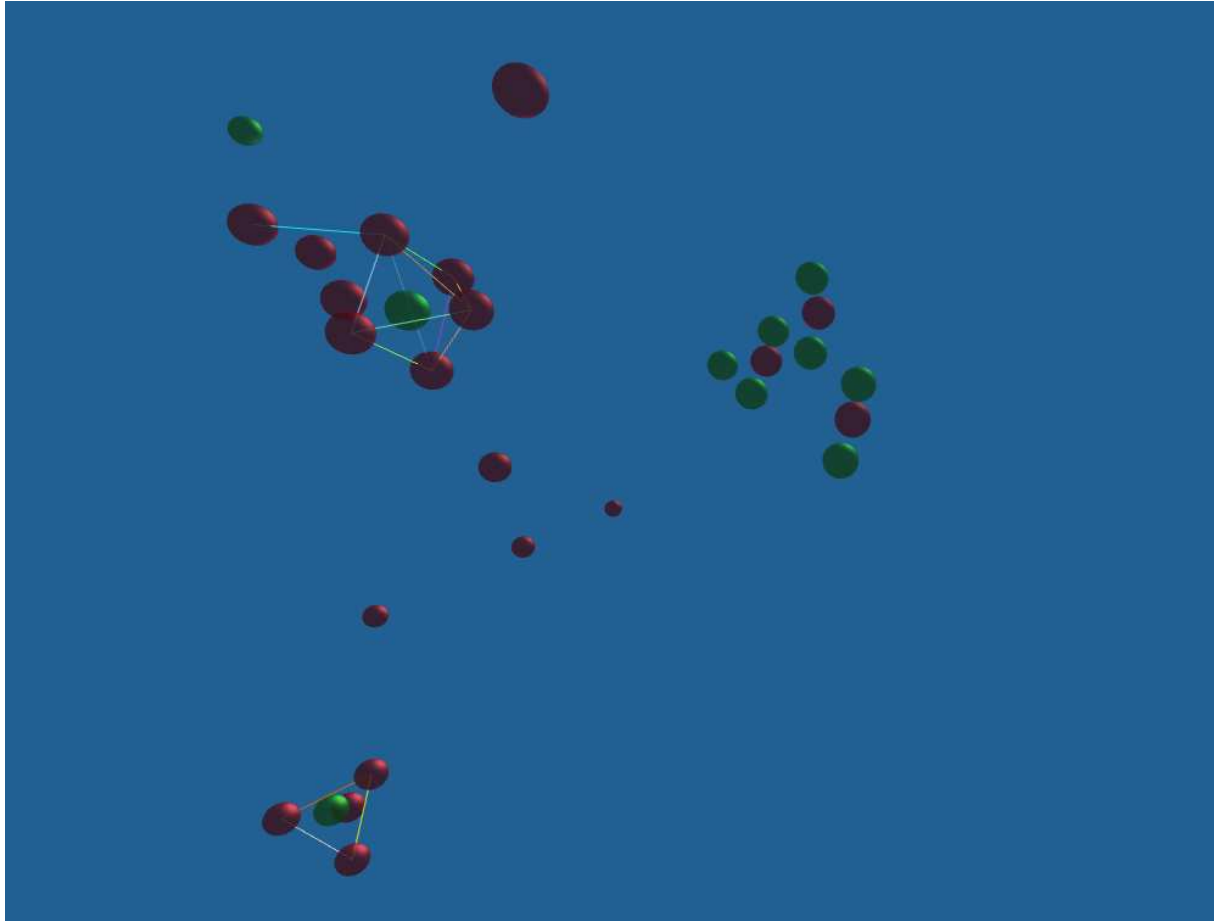


Fig. 9. A picture of the Frenkel pairs in Cu at PKA energy of 2 keV. Vacancies are in red and the interstitials are in green color. Note that dumbbells and complex vacancy clusters are common in Cu, even at low energies of PKA.

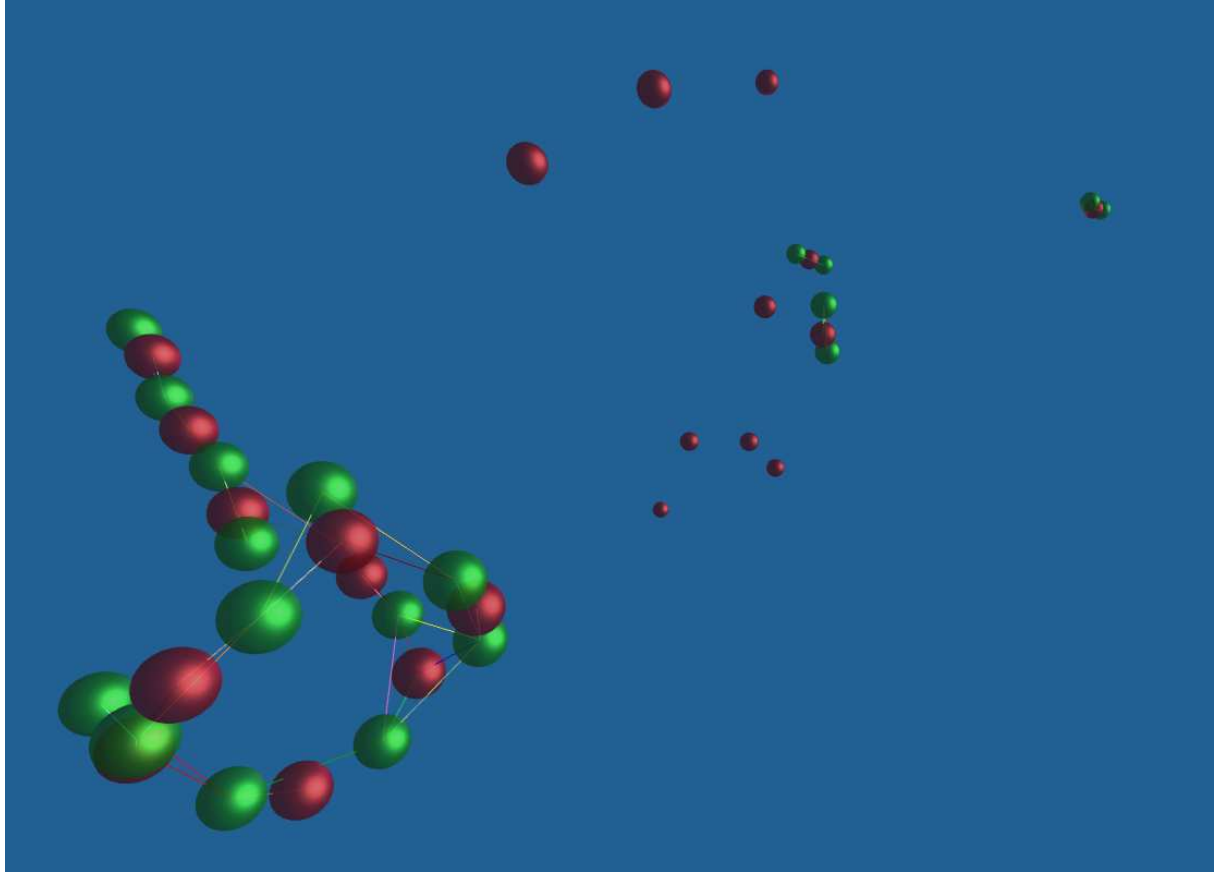


Fig. 10. A picture of the Frenkel pairs in W at PKA energy of 5 keV. Vacancies are in red and the interstitials are in green color. It shows dumbbells, crowdions and ring like arrangement of interstitial clusters.

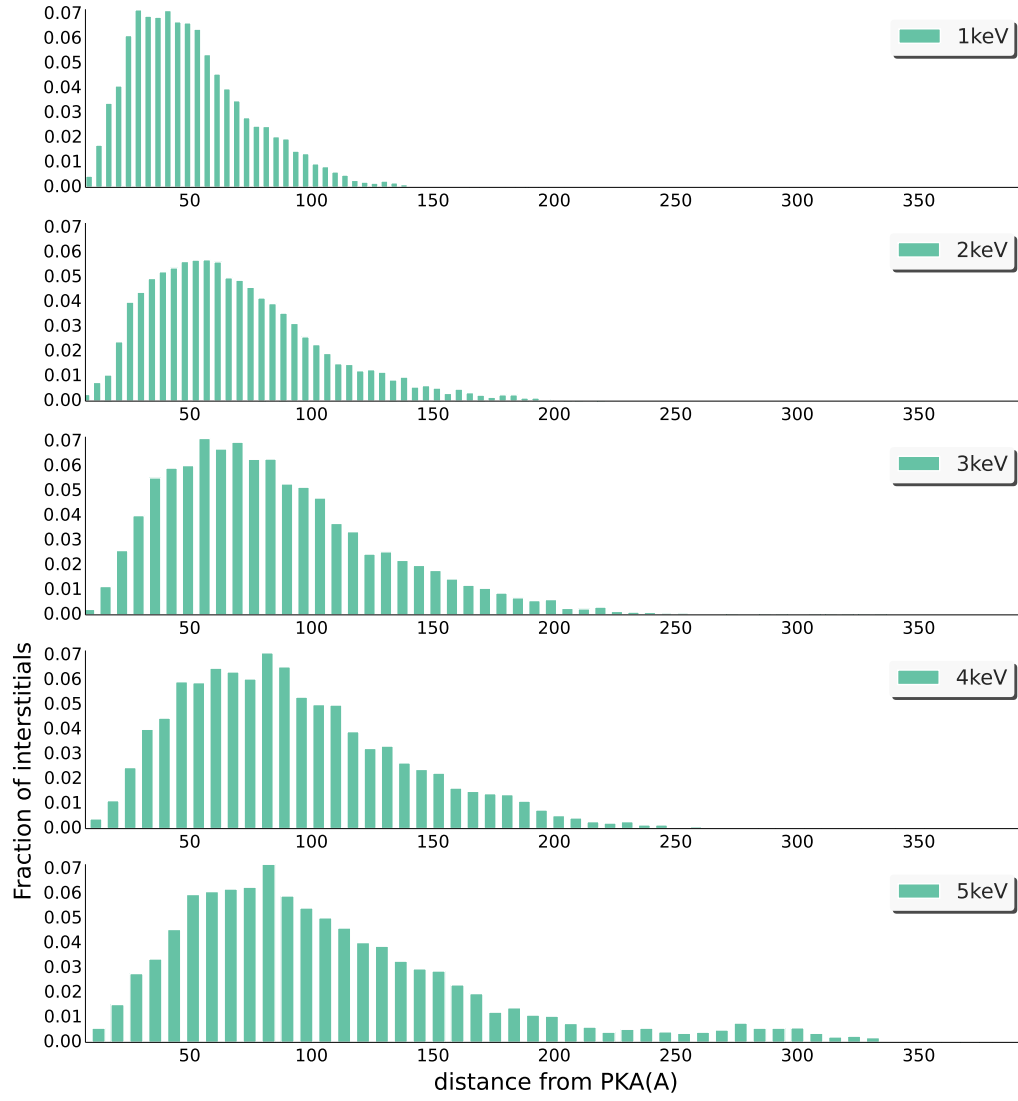


Fig. 11. Distribution of the interstitials as a function of distance from the origin of the PKA for energies 1-5 keV in Cu

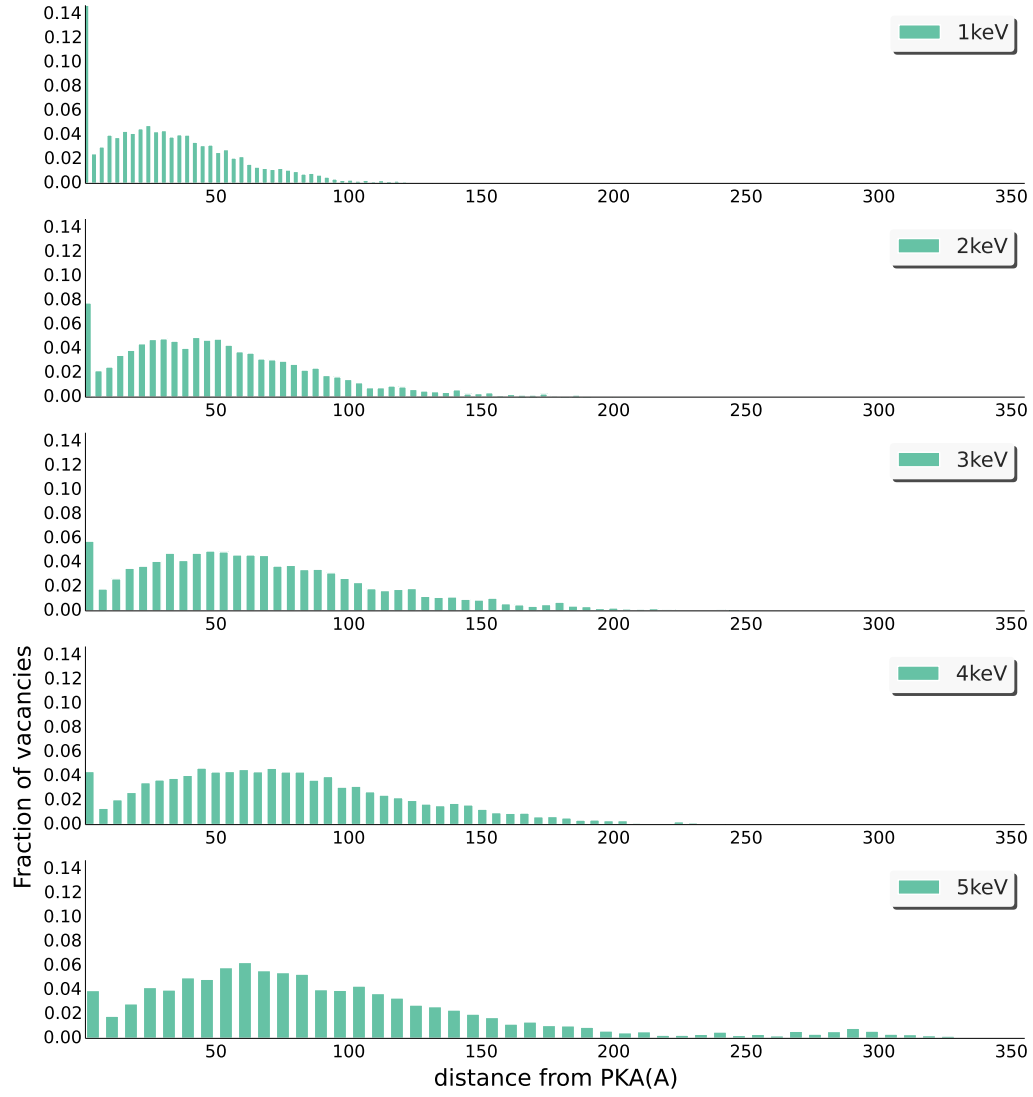


Fig. 12. Distribution of the Vacancies as a function of distance from the origin of the PKA for energies 1-5 keV in Cu

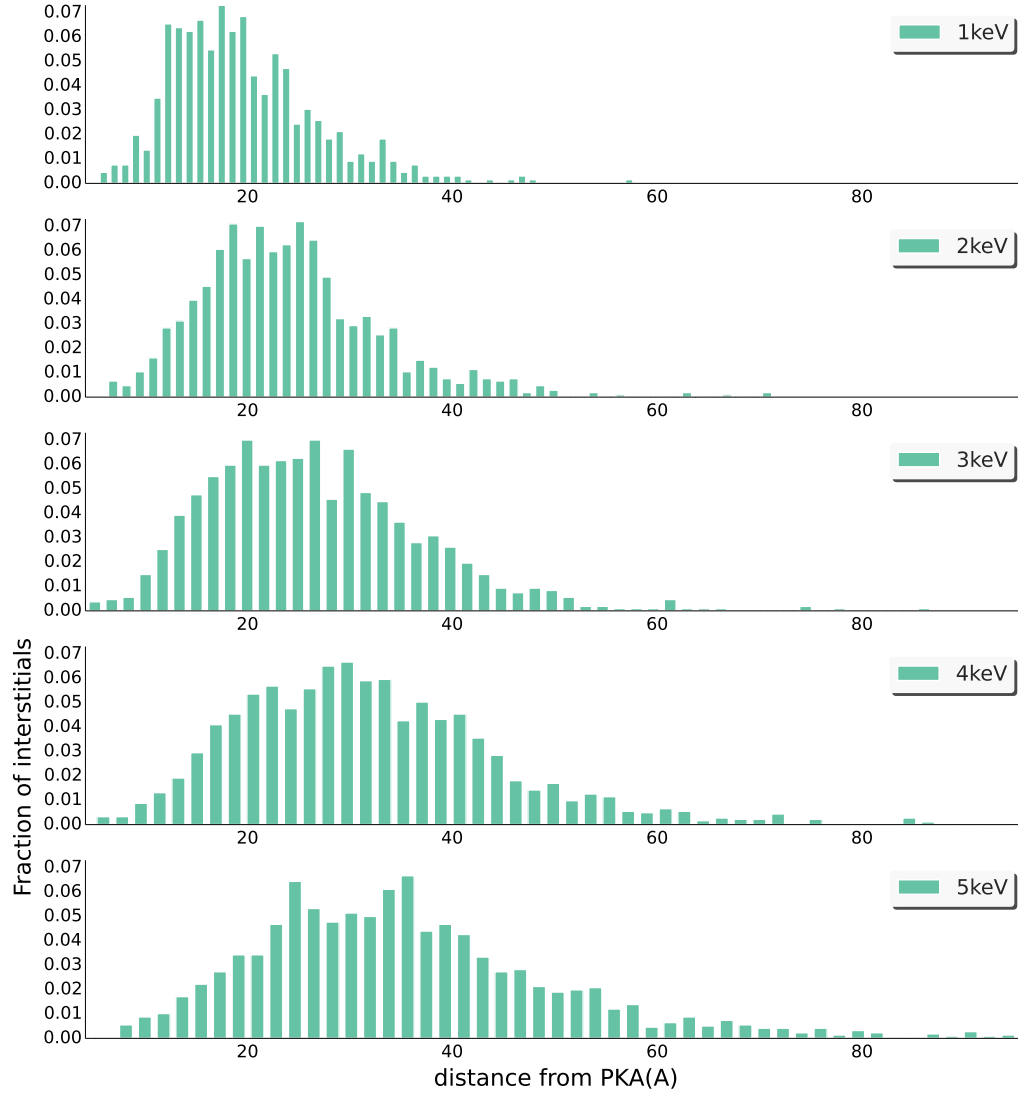


Fig. 13. Distribution of the interstitials as a function of distance from the origin of the PKA for energies 1-5 keV in W

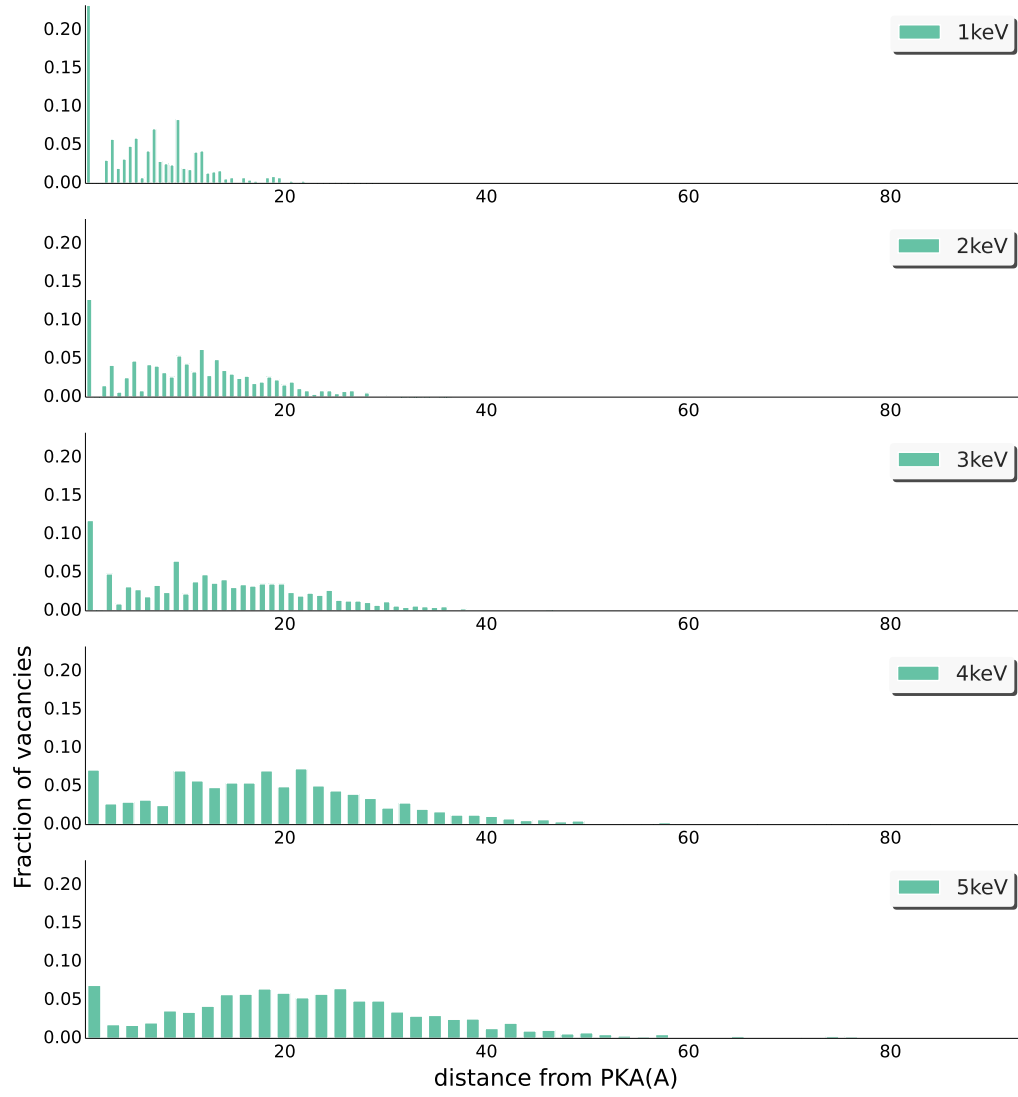


Fig. 14. Distribution of the Vacancies as a function of distance from the origin of the PKA for energies 1-5 keV in W

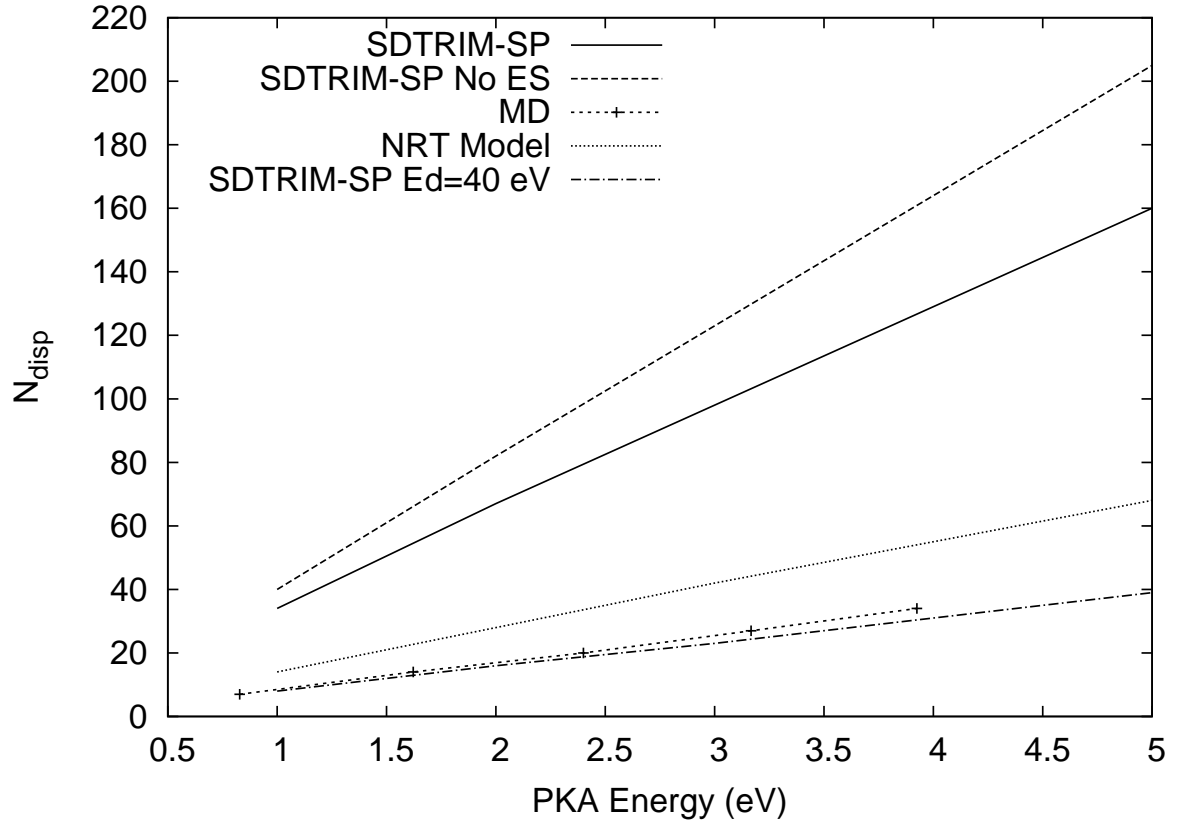


Fig. 15. Variation of the number of Frenkel Pairs as a function of the energy of PKA from MD simulations, NRT Model and SDTRIM-SP simulations for the three cases, viz. without electronic stopping, with electronic stopping, with $E_d = 40$ eV for Cu

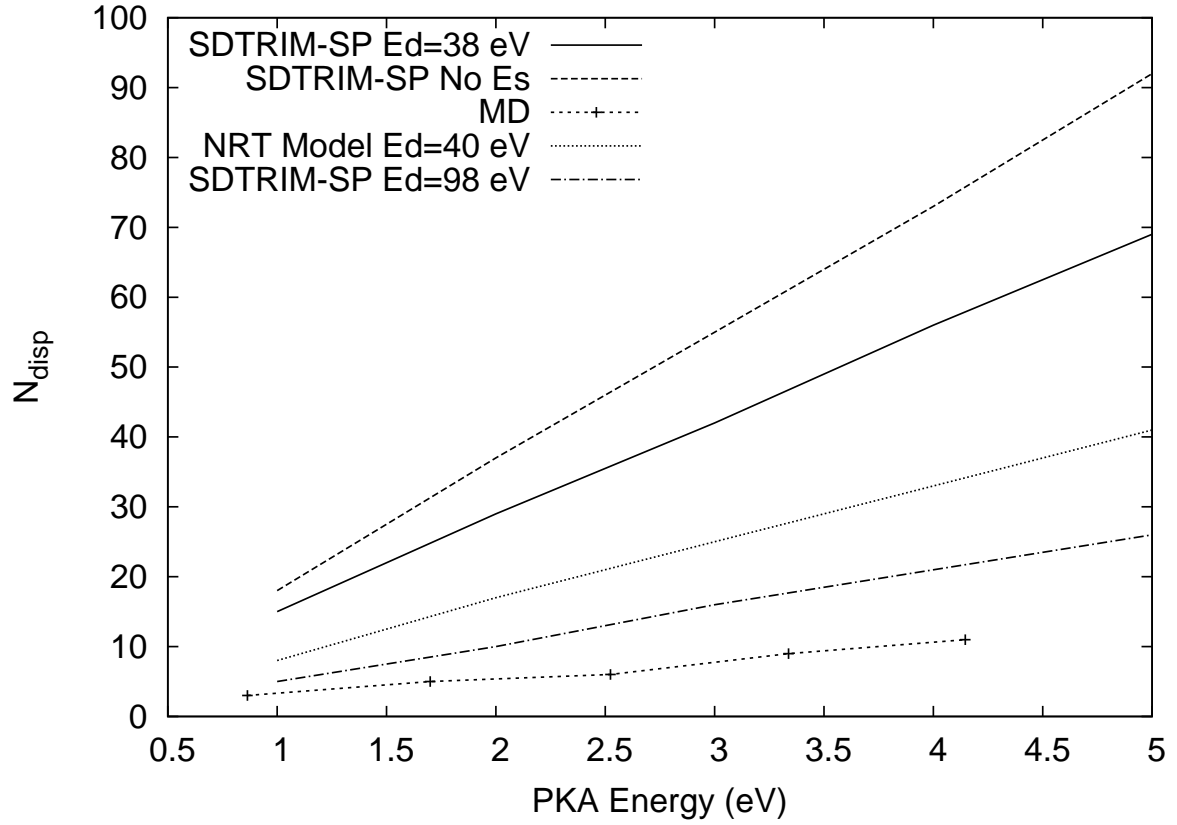


Fig. 16. Variation of the number of Frenkel Pairs as a function of the energy of PKA from MD simulations, NRT Model and SDTRIM-SP simulations for the three cases, viz. without electronic stopping, with electronic stopping, with $E_d = 98$ eV for W